An Anisotropic Vector Hysteresis Model of Grain-Oriented Steels

Yating Li[1,2], Jun Liu[2], Yongjian Li[1*], Shuaichao Yue[1], Ruiying Chen[3], Christopher Harrison[2], Philip Anderson[2]
[1]State Key Laboratory of EERI, Hebei University of Technology, 300130, Tianjin, China, liyatingtt@163.com, liyongjian@hebut.edu.cn, 2023921@hebut.edu.cn.
[2]School of Engineering, Cardiff University, Cardiff CF24 3AA, U.K, liuj118@cardiff.ac.uk, harrisonc15@cardiff.ac.uk, andersonpi1@cardiff.ac.uk.
[3]Department of Electrical Engineering, Tsinghua University, Beijing 100190, China, 415801646@qq.com.

This paper presents a vector hysteresis model that characterizes the anisotropic behavior of grain-oriented (GO) electrical steel. The anisotropic anhysteresis model with permeability tensors that considers crystallographic orientation based on magnetic domain theory is developed. An additional easy axis aligned with the direction of the applied magnetic field is introduced for anisotropy near saturation. The hysteresis behavior is modeled through the association of the anhysteresis model and energy-based model. Material parameters for both reversible and irreversible behaviors are identified through experimental characterization performed on B27R090 electrical steel under different magnetization directions. Comparisons between experimental and calculated hysteresis loops, as well as iron losses, validate the models accuracy.

***Index Terms*—Magnetic hysteresis, magnetic materials, magnetic anisotropy, magnetic losses**

I. Introduction

The magnetic properties of GO electrical silicon steels, such as hysteresis loops, losses, and permeability, exhibit significant anisotropy. This behavior arises from the strong anisotropy of Iron-Silicon crystals, coupled with the highly pronounced crystallographic texture of the material [1]. GO steels are widely utilized in electromagnetic devices such as power transformers and large rotating machines [2]. While standard characterization typically focuses on the rolling (RD) and transverse (TD) directions, practical applications, such as transformer cores, often involve magnetization in other directions. Developing physics-based models that account for anisotropy effects in magnetization processes is essential for accurate characterization of materials.

Various anisotropic hysteresis models have been developed to characterize the magnetic anisotropy and hysteresis effects of electrical steels, primarily based on macroscopic measurements. These models can generally be classified into two categories. The first category involves superposing scalar models distributed in possible directions, for instance, the vector model proposed by Mayergoyz [3]. The second category vectorizes the model by integrating intrinsic vector elements, such as in the vector Jiles-Atherton (JA) model [4]. However, the lack of physical meaning and link to microstructures significantly limits the accuracy and generality of the model. Although the multiscale model presented in [5] accounts for polycrystalline texture, it does not provide a detailed analysis of domain distribution evolution during the magnetization process. This paper proposes an anisotropic hysteresis model that considers the distribution of elementary magnetic domains and crystallographic orientation. The validity of the proposed model is demonstrated through comparisons with measured hysteresis loops under different magnetization directions.

II. The Anhysteresis Magnetization Modelling

Based on the assumption proposed by Bozorth [6], a cubic crystal is composed of a large number (N) of elementary magnetic domains with equal size. They can only orient along one of the magnetic easy axes, defined as N_i (i=1-6). The number of domains oriented in the [100] direction is N_1, for the domains oriented in [$\bar{1}$00] it is N_2, etc. Considering the influence of Zeeman energy on the magnetic domain distribution near saturation, we introduce an additional easy axis aligned with the direction of the applied magnetic field $\boldsymbol{H}$. The magnetic domain distribution along this axis is represented by N_7. For an iron crystal with Goss texture, the assumed orientation of the easy axes and the corresponding coordinate system is illustrated in Fig. 1. The magnetic flux density in crystal coordinate $\boldsymbol{B}$ is determined using the following equation:

$$\boldsymbol{B}=\begin{bmatrix}B_x\\B_y\\B_z\end{bmatrix}=\begin{bmatrix}(N_1-N_2+N_7\gamma_x)B_s/N\\(N_3-N_4+N_7\gamma_y)B_s/N\\(N_5-N_6+N_7\gamma_z)B_s/N\end{bmatrix}, \quad (1)$$

where B_x, B_y and B_z are the components of $\boldsymbol{B}$ along the x-, y- and z- axes, γ_x, γ_y and γ_z are the direction cosines of the $\boldsymbol{H}$ in crystal coordinate, and B_s represents the saturation magnetic flux density.

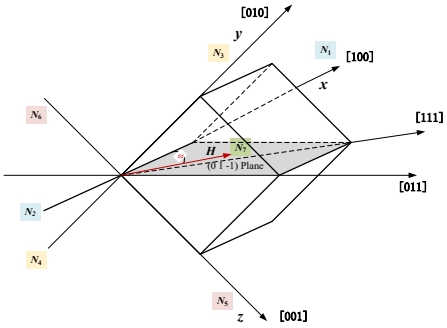


Fig.1. The orientation of iron crystals in Goss texture.

The distribution of N_i (i=1-7) is obtained by minimizing the energy E_{min}, which includes the Zeeman energy E_z and crystalline anisotropy energy E_c, as expressed as:

$$\begin{aligned}E_c &= NK_0+N_7[K_1(\gamma_x^2\gamma_y^2+\gamma_y^2\gamma_z^2+\gamma_z^2\gamma_x^2)+K_2\gamma_x^2\gamma_y^2\gamma_z^2];\\ E_z &= -[(N_1-N_2)\gamma_x+(N_3-N_4)\gamma_y+(N_5-N_6)\gamma_z;\\ &\quad +N_7]HB_s\\ E_{\min} &= (E_c+E_z)/N\end{aligned} \quad ,(2)$$

where K_0, K_1, and K_2 are the anisotropy constants. In the process of solving the minimum energy, the distribution of N_i should

satisfy the following constrains:

$$N_1 + N_2 + N_3 + N_4 + N_5 + N_6 + N_7 = N\,, \tag{3}$$

$$\boldsymbol{B} = \mu_0 \boldsymbol{\mu}_r \boldsymbol{H}\,. \tag{4}$$

The sum of the calculated N_i (i=1-7) equals the constant N as expressed in (3). The calculated magnetic flux density $\boldsymbol{B}$, applied magnetic field $\boldsymbol{H}$, and relative permeability tensor $\boldsymbol{\mu}_\mathbf{r}$ satisfy the constitutive relation given in (4). μ_0 is the vacuum permeability. The permeability tensor $\boldsymbol{\mu}_\mathbf{r}$ considering the crystallographic texture and domain configuration is expressed as [7]:

$$\boldsymbol{\mu} = \boldsymbol{g}^{-1}[\frac{1}{N}\sum_{i=1}^{7} N_i \boldsymbol{\mu}_i]\boldsymbol{g}\,, \tag{5}$$

where $\boldsymbol{g}$ is the crystallographic orientation matrix, $\boldsymbol{\mu}_i$ is the relative elementary permeability for the domains in each easy direction, defined as:

$$\begin{aligned} \boldsymbol{\mu}_1 &= \boldsymbol{\mu}_2 = diag(\mu_c, 1, 1); \\ \boldsymbol{\mu}_3 &= \boldsymbol{\mu}_4 = diag(1, \mu_c, 1); \\ \boldsymbol{\mu}_5 &= \boldsymbol{\mu}_6 = diag(1, 1, \mu_c); \\ \boldsymbol{\mu}_7 &= diag(\gamma_x \mu_{N_7}, \gamma_y \mu_{N_7}, \gamma_z \mu_{N_7}) \end{aligned}\,, \tag{6}$$

where μ_c is the relative elementary permeability of a domain along the six easy axes, while μ_{N7} denotes the relative elementary permeability of a domain along the direction of $\boldsymbol{H}$. The flow chart of the model is as follows:

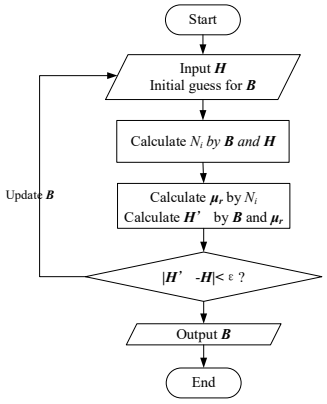


Fig.2. Flow chart of the proposed anhysteresis model.

III. The Vector Hysteresis Model

The EB (Energy based) model with dry-friction-like hysterons is used to describe the hysteresis properties of magnetic material. The applied magnetic field $\boldsymbol{H}$ is decomposed into a reversible part $\boldsymbol{H}_{\mathrm{re}}$ and an irreversible part $\boldsymbol{H}_{\mathrm{ir}}$:

$$\boldsymbol{H} = \boldsymbol{H}_{re} + \boldsymbol{H}_{ir}\,. \tag{7}$$

The reversible field $\boldsymbol{h}_{\mathrm{re}}$ for a single hysteron at each calculation step is updated as [8]:

$$\boldsymbol{h}_{re} = \begin{cases} \boldsymbol{H} - H_{ir}\dfrac{\boldsymbol{H} - \boldsymbol{h}_{re}}{|\boldsymbol{H} - \boldsymbol{h}_{re}|} & \text{if } \left|\boldsymbol{H} - \boldsymbol{h}_{re}^{\,P}\right| \geq H_{ir} \\ \boldsymbol{h}_{re} & \text{otherwise} \end{cases}\,, \tag{8}$$

where $\boldsymbol{h}_{\mathrm{re}}^{\,P}$ is the calculated result at the previous step. The output of all hysterons with normalized weighted $\omega(\kappa)$ are summed together to obtain the total reversible field $\boldsymbol{H}_{\mathrm{re}}$:

$$\boldsymbol{H}_{re} = \sum_{n=1}^{N_h} \boldsymbol{h}_{re}^{\,n} \varpi(\kappa_n) \tag{9}$$

where N_{h} is the number of hysterons. The reversible field $\boldsymbol{H}_{\mathrm{re}}$ is the input of the anhysteresis model in Section II to involve the anisotropy effect into the model.

IV. Experiment and Validation

The crystallographic orientation of grain-oriented GO electrical steel follows the Goss structure, and due to its highly uniform grain alignment, it can be approximated using a single-crystal model to calculate its magnetic properties. The calculated anhysteresis curves are presented in Fig. 3(a). The magnetic properties of B27R090 in different magnetization directions are measured by a 2-D measurement system. The detailed introduction of the system can be found in [9]. An example of the dataset used for parameter identification is shown in Fig.3 (b). Further details on parameter identification and validation will be provided in the full paper.

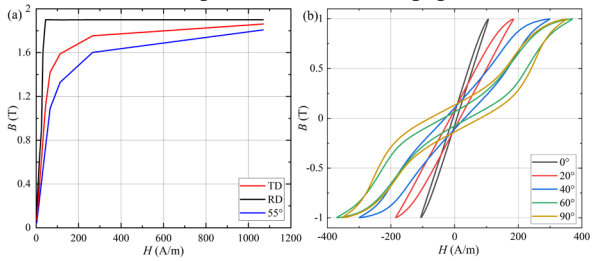


Fig. 3. (a) Calculated anhysteresis curves along RD, TD and 55°. (b) Measured hysteresis loops along different magnetization directions.

V. Conclusion

An anisotropic hysteresis model is developed to evaluate the magnetic anisotropy of GO electrical steels. The model considers anisotropy arising from crystallographic orientation based on domain configuration. The model can be extended to polycrystalline steels modelling by incorporating the orientation distribution function (ODF). Hence, both local and global anisotropy for typical textures can be captured.

References

[1] A. P. S. Baghel, M. Enokizono, and K. Fujiwara, "Hysteresis modelling of GO laminations for arbitrary in-plane directions taking into account the dynamics of orthogonal domain walls," J. Magn. Magn. Mater., vol. 418, pp. 14–20, Oct. 2016.

[2] F. Fiorillo, C. Ragusa, and M. Pasquale, "Comprehensive model of magnetization curve, hysteresis loops, and losses in any direction in grain-oriented Fe-Si," IEEE Trans. Magn., vol. 38, no. 3, pp. 1467–1476, Mar. 2002.

[3] I. Mayergoyz, Mathematical Models of Hysteresis and Their Applications. Elsevier, 2003.

[4] B. Upadhaya, P. Rasilo, L. Perkkiö, P. Handgruber, A. Benabou, A. Belahcen, and A. Arkkio, "Alternating and rotational loss prediction accuracy of vector Jiles-Atherton model," J. Magn. Magn. Mater., vol. 527, 167690, Jun. 2021.

[5] L. Daniel, O. Hubert, N. Buiron, and R. Billardon, "Reversible magneto-elastic behavior: A multiscale approach," J. Mech. Phys. Solids, vol. 56, no. 3, pp. 1018–1042, Mar. 2008.

[6] R. M. Bozorth, "The theory of the ferromagnetic anisotropy of single crystals," Phys. Rev., vol. 42, no. 6, pp. 882–897, Dec. 1932.

[7] J. Liu and C. Davis, "Tensorial permeability microstructure model considering crystallographic texture and grain size for evaluation of magnetic anisotropy in polycrystalline steels," Philos. Mag., vol. 101, no. 10, pp. 1224–1244, Mar. 2021.

[8] R. Chen, Y. Zhang, and L. Zhou, "An energy-based anisotropic vector hysteresis model for rotational electromagnetic core loss," IEEE Trans. Ind. Electron., vol. 71, no. 6, pp.6084-6094, Jun. 2023.

[9] S. Yue, J. Zhou, and H. Zhu, "Measurement and analysis of the non-symmetry of transverse magnetisation and resulting loss in grain-oriented steel using a modified RSST," J. Magn. Magn. Mater., vol. 561, 169671, Nov. 2022.